Research article

Design and synthesis of fatty acid derived 4-methoxybenzylamides as antimicrobial agents

Zubair Rehman Nengroo [a,*], Aijaz Ahmad [b], Adil Tantary [c], Adil Shafi Ganie [d], Zeshan Umar Shah [e]

[a] Department of Chemistry, Aligarh Muslim University, Aligarh 202002, India
[b] Department of Biochemistry, Aligarh Muslim University, Aligarh 202002, India
[c] Department of Botany, Aligarh Muslim University, Aligarh 202002, India
[d] Environmental Chemistry Section, Department of Chemistry Aligarh Muslim University, Aligarh 202002, India
[e] Department of Zoology, Aligarh Muslim University, Aligarh 202002, Uttar Pradesh, India

ABSTRACT

A new series of fatty acid amides viz. N-(4-methoxybenzyl)undec-10-enamide (5), (9Z, 12R)-12-Hydroxy-N-(4-methoxybenzyl)octadec-9-enamide (6) and N-(4-methoxy benzyl)oleamide (7) were synthesized by using a suitable synthetic route involving DCC and DMAP as catalysts. The synthesized compounds were characterized through FTIR, NMR spectroscopy, and mass spectrometry. DNA binding studies through spectroscopy and molecular docking were performed to evaluate the binding mechanism of molecules (5–7) with (ctDNA). The inhibition zone with reference to standards, Minimum Inhibitory Concentration (MIC) and Minimum Killing Concentration (MKC) values were determined to study the in vitro antimicrobial activity for tested compounds. Among all the tested compounds, the compound 6 containing hydroxy group at the fatty acid chain showed most powerful antifungal as well as antibacterial activity.

1. Introduction

Infection due to microbes has become a serious health hazard and has posed grave threat to health care systems. Therefore, development of antimicrobial agents to treat various infections is an interesting area of contemporary research. The increased drug resistance in microbes leads to severe implications such as higher mortality and morbidity (Devasia et al., 2006). The enteric bacterial infection is one of the major problems in developing countries: Indian-subcontinent and some tropical parts of South Africa (Zhang et al., 2006). The world's most common and dreadful infectious diseases like dysentery and diarrhea were mainly caused by Escherichia coli (E. coli) (Puerto et al., 2006; Yoder et al., 2006). Various synthesized drugs containing an Azole and bile acid derived oxazole functionalities have been used against fungal diseases (Fernandez et al., 2016; Shafiei et al., 2020). The E. coli can be treated with Amoxicillin, Norfloxacin and Ciprofloxacin, but they generally have some side effects (Nolan et al., 1979). Bacterial resistance and drug toxicity are the major drawbacks for the treatment of these infections (Li and Webster, 2018). A huge number of diseases are caused by gram-positive and gram-negative bacteria that results in the damage to host tissue (Ramachandran, 2014).

Till date several seed extracts, fatty acids and their derivatives have been tested to know their antibacterial (Nengroo and Rauf, 2019, 2020), antifungal (Nengroo et al., 2020), and antioxidant (Nengroo and Rauf, 2019) activities. However, FA-Amide analogs have received very little attention as antimicrobial agents despite of the fact that these molecules possess a broad range of biological activities. These FA-Amide analogs have shown excellent activity to treat obesity, diabetes, cancer, cardiovascular diseases, inflammation, pain, drug addiction, eating disorders, anxiety, depression and CNS disorders (Witkamp, 2010; Di Marzo et al., 2007; Starowicz et al., 2007; Karanian and Bahr, 2006; Felder et al., 2006; Ahn et al., 2009; Adelani and Labunmi, 2017).

DNA, an important genetic substance plays an extremely and significant role in the process of gene expression, gene transcription, mutagenesis, and carcinogenesis within an organism (Kathiravan and Renganathan, 2009). The main target molecule for natural and synthetic molecules is DNA. In recent past the study of some organic compounds like pesticides have been the focus among researchers across the world, owing there potential of being genotoxic as well as alkylating agents for DNA molecules (Zhang et al., 2012). Previous studies have shown that pesticides covalently bind and intercalate to DNA molecules and develop

* Corresponding author.
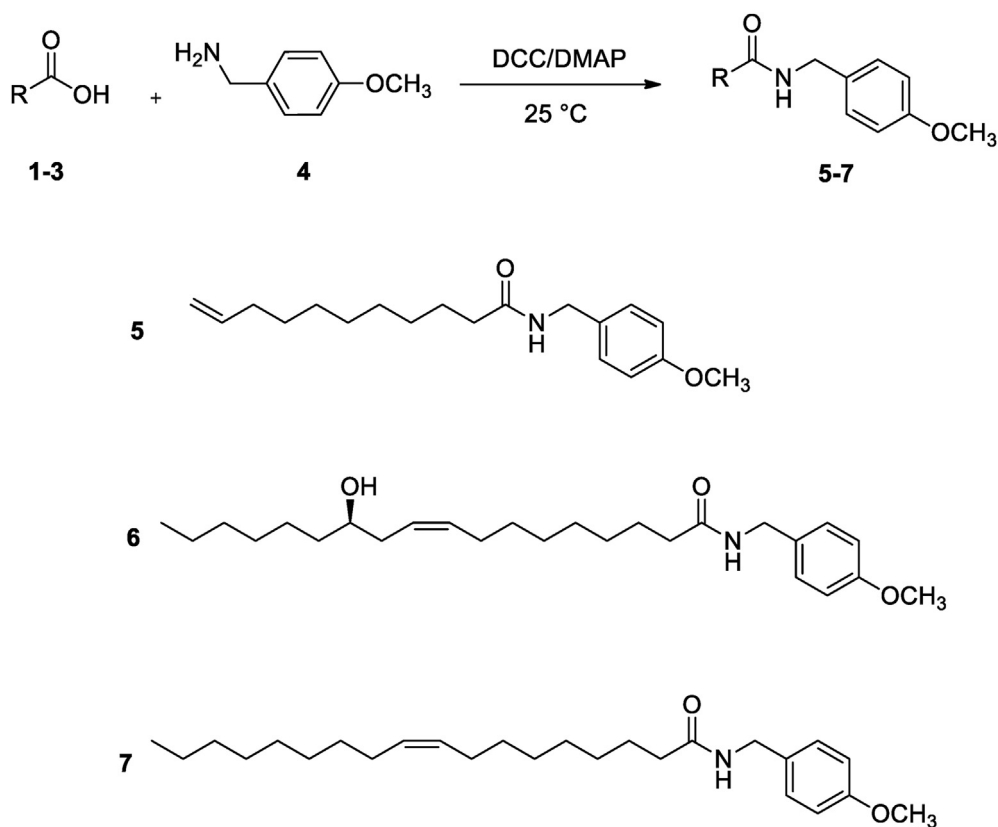E-mail address: zubairchem33@gmail.com (Z.R. Nengroo).

Figure 1. Synthesis of fatty acid amides of 4-methoxybenzylamine using DCC/DMAP as a catalyst.
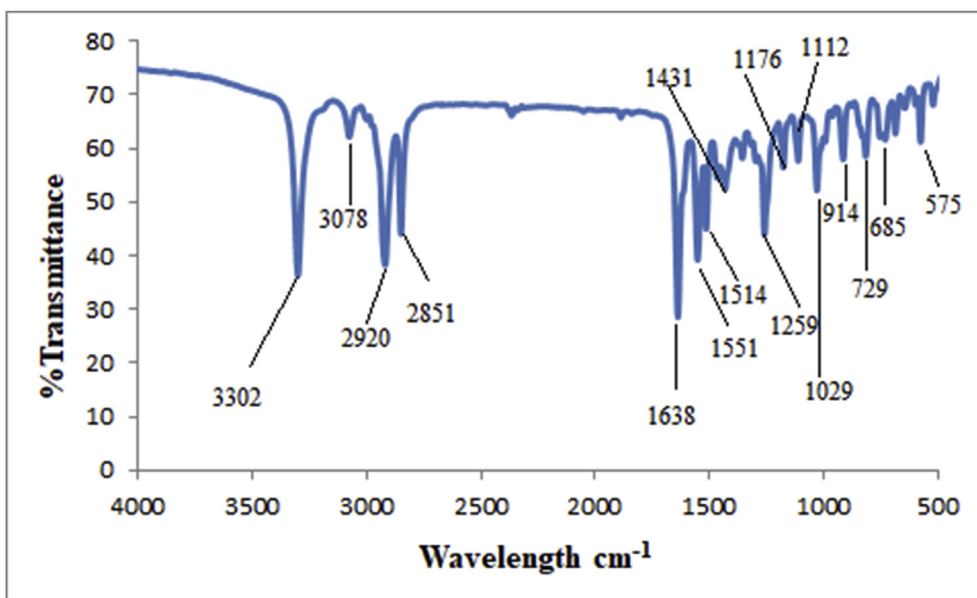

Figure 2. FTIR analysis of *N*-(4-methoxybenzyl)undec-10-enamide (Compound 5).

adducts, which leads to mutation and start potential carcinogenic effects (Saquib et al., 2010). Generally the small compounds bind to the DNA by three non-covalent ways: intercalation, groove binding, and electrostatic interaction (Tjahjono et al., 1999). Intercalative and groove binding occurs in the grooves of the DNA, while electrostatic binding occurs out of the DNA groove. Among all the most effective modes intercalative binding is considered as most effective mode of DNA modification by chemical target (Tan et al., 2009). There are several methods (Zhang et al., 2014) for the preparation of FA-Amides, The N,

N-dicyclohexylcarbodiimide (DCC) as a coupling agent marked first mild method for synthesis of FA-amides and esters (Sheehan and Hess, 1955). Our laboratory also working in the field of natural product, particularly, isolation, characterization, derivatization of fatty acids (Ahmad et al., 2013; Banday et al., 2010). The main aim of this work was to find the novel bioactivity of various FA-amide derivatives of 4-Methoxybenzylamine (PMBA). Keeping into consideration the potential of FA as pharmacophores, here we report the design, synthesis, and *in vitro* evaluation of FA-amide of PMBA derivatives as antimicrobial agent.
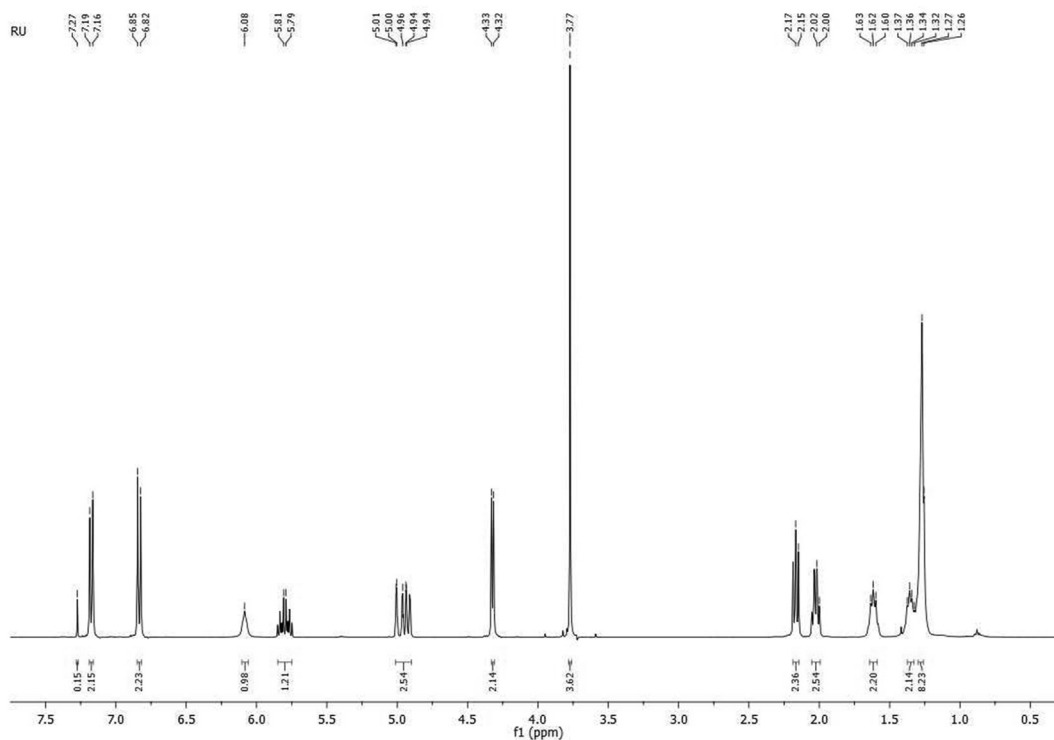
RU   7.27 7.19 7.16   6.85 6.82   6.08   5.81 5.79   5.01 5.00 4.96 4.94 4.94   4.33 4.32   3.77   2.17 2.15 2.02 2.00   1.63 1.62 1.60 1.37 1.36 1.34 1.32 1.27 1.26

0.15 2.15   2.23   0.98   1.21   2.54   2.14   3.62   2.36 2.54   2.20   2.14 8.23

7.5   7.0   6.5   6.0   5.5   5.0   4.5   4.0   3.5   3.0   2.5   2.0   1.5   1.0   0.5
f1 (ppm)

Figure 3. ^{1}H NMR analysis of *N*-(4-methoxybenzyl)undec-10-enamide (Compound 5).

173.07   158.92   139.16   130.60 129.12   114.18 113.99   77.45 77.13 76.81   55.26   42.95   36.73 33.80 29.71 29.35 29.32 29.08 28.90 25.80

170   160   150   140   130   120   110   100   90   80   70   60   50   40   30   20
f1 (ppm)
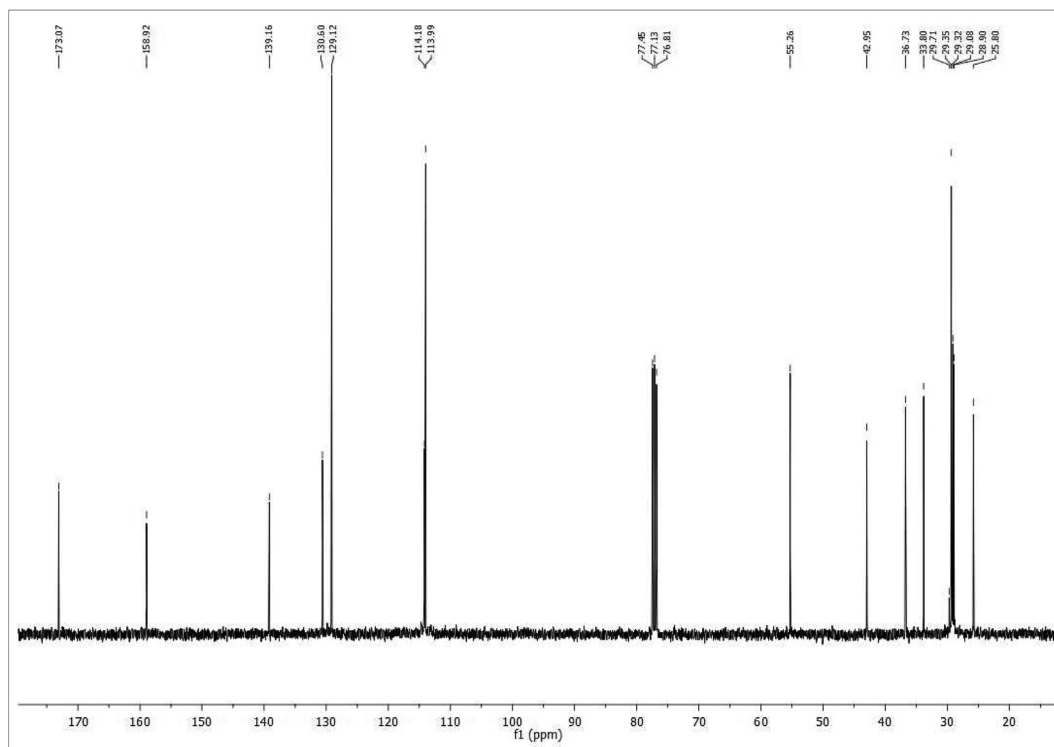
Figure 4. ^{13}C NMR analysis of *N*-(4-methoxybenzyl)undec-10-enamide (Compound 5).

2. Materials and methods

2.1. Chemicals, reagents and instruments

(9Z)-octadec-9-enoic (97%) and Undec-10-enoic (98%) acids were purchased from fluka chemicals (Bucks, Switzerland). The 4-Methoxybenzylamine was purchased from TCI chemicals (India) Pvt. Ltd. All the solvents used were of analytical grade. The glass plates with layer of silica gel (0.5 mm, Merck, Mumbai, India) were used for thin layer chromatography (TLC). Highly polymerized Calf thymus DNA (ctDNA) was obtained from Sigma Aldrich. Hoechst33342 was obtained from Life Technologies, USA. Ethidium bromide (EtBr) was purchased
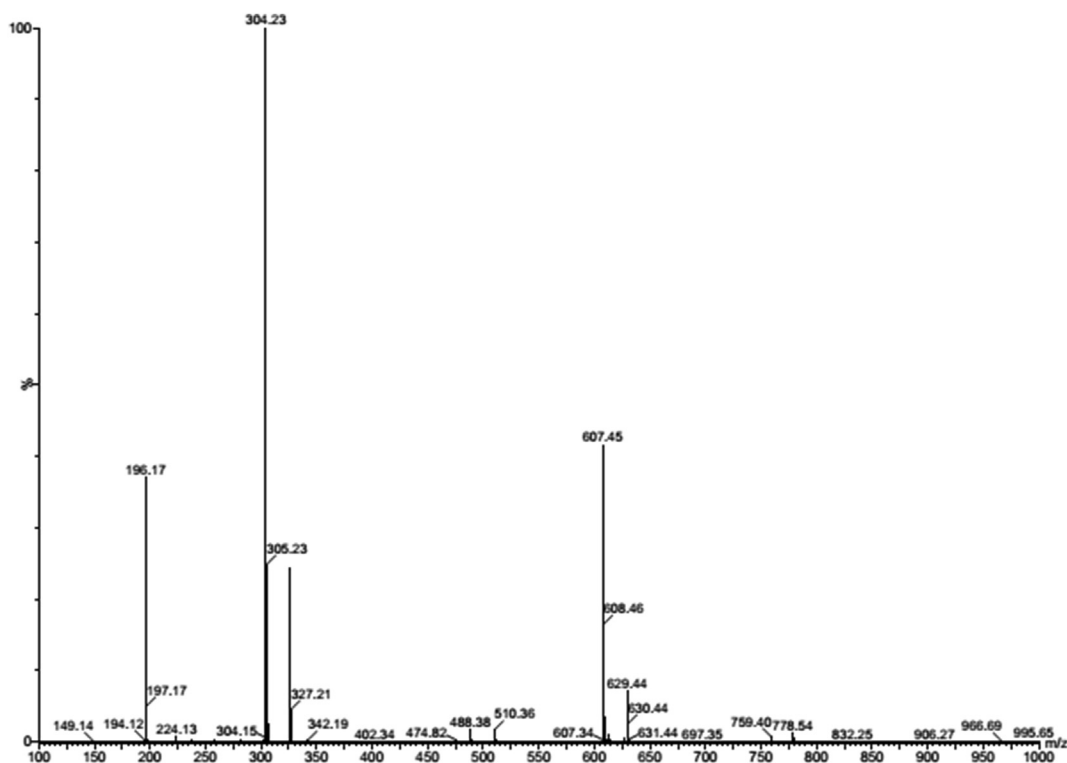
Figure 5. ESI-MS analysis of *N*-(4-methoxybenzyl)undec-10-enamide (Compound 5).
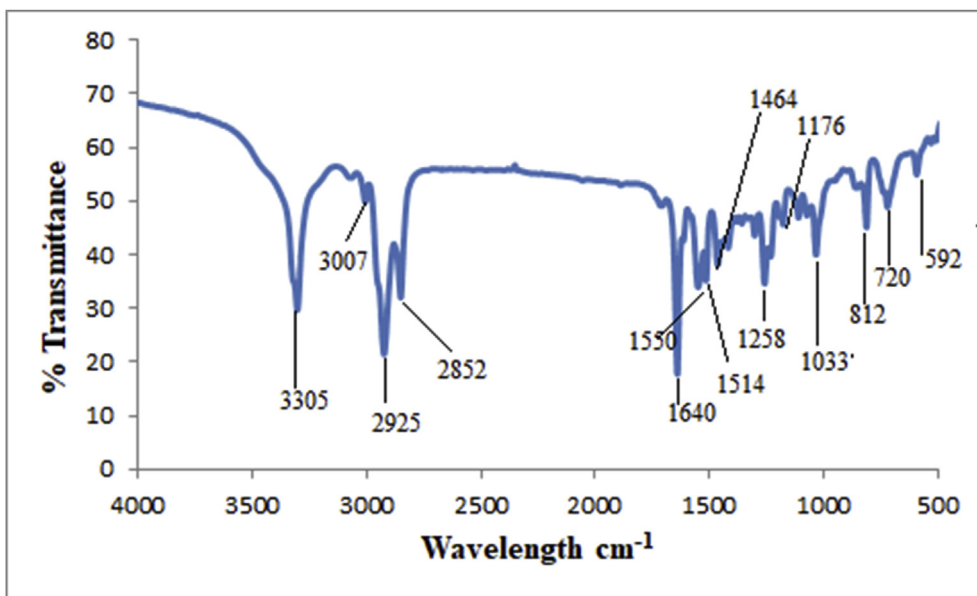

Figure 6. FTIR analysis of (*R,Z*)-12-hydroxy-N-(4-methoxybenzyl)octadec-9-enamide (Compound 6).

from SRL. Tris–HCl buffer medium (10 mM) at pH 6.8 was used as medium for conducting experiments. The EtBr (0.1 mM) and HO stock solutions (0.15 mM) after being prepared by dissolving their crystals in a Tris–HCl buffer solution have been stored in a cool and dark place. Column chromatography was conducted using silica gel (Merck, Mumbai, India) having mesh size of 60–120. The Shimadzu 8201 PC spectrometer was used to record IR spectra and absorption as given in cm-1. 13C NMR and 1H NMR were recorded in Bruker DRX-400 instrument in CDCl3. TMS was used as an internal standard, and chemical shifts (δ) were measured relative to TMS and quoted in ppm. Coupling constants (*J*) are expressed in Hertz (Hz). The JEOL-SX 102/DA-600 Mass

spectrometer was used to record mass spectra. Melting points are taken in an open capillary and are uncorrected.

2.2. General synthesis for fatty acid derived 4-methoxybenzylamides

(9*Z*, 12*R*)-12-Hydroxyoctadec-9-enoic (ricinoleic, 98%) acid was isolated from *Ricinus communis* (*R. communis*) seed oils, following the method of Gunstone (1954), further purified by column chromatography. A solution of FA (5 mmol), DCC (5.5 mmol) and MBA (5 mmol) in dichloromethane (40 ml) was taken in a dried conical flask, catalytic amount of DMAP was added, and the reaction was stirred
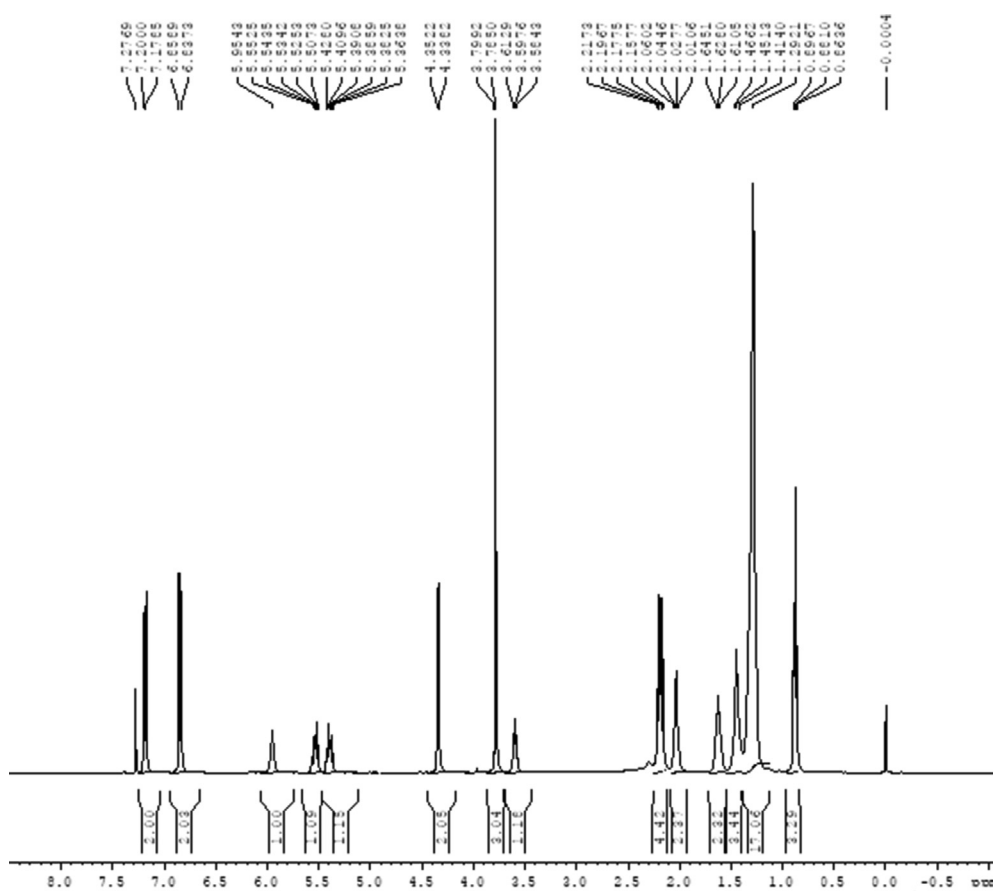
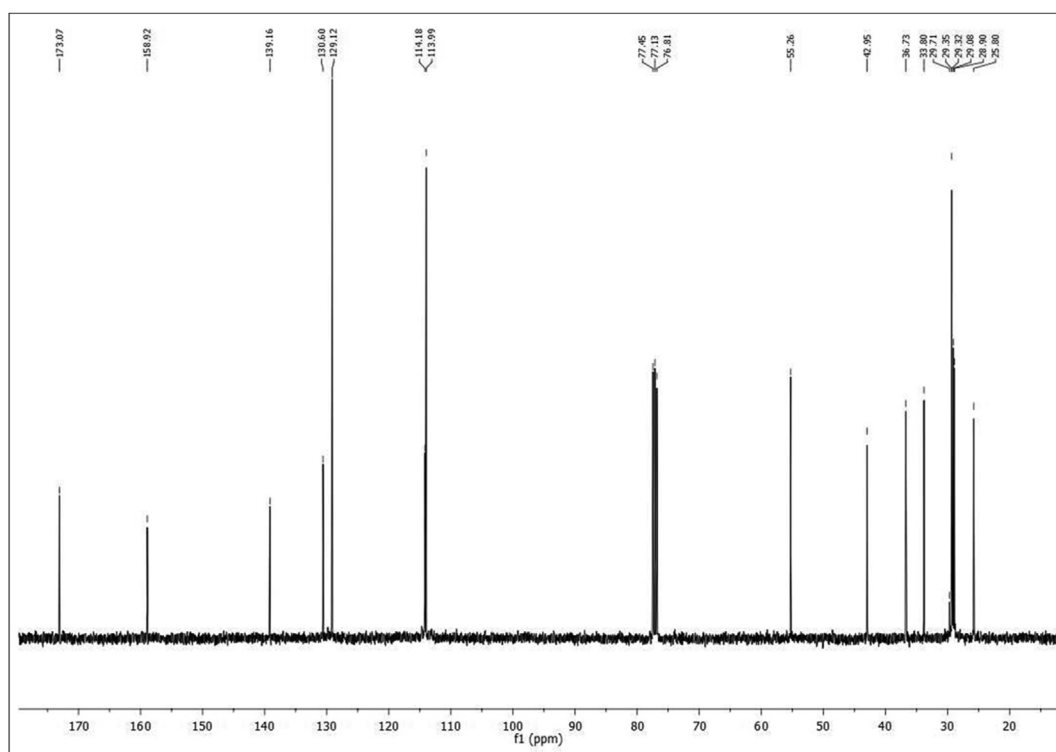**Figure 7.** ^{1}H NMR analysis of (*R,Z*)-12-hydroxy-N-(4-methoxybenzyl)octadec-9-enamide (Compound 6).

Figure 8. ^{13}C NMR analysis of (*R,Z*)-12-hydroxy-N-(4-methoxybenzyl)octadec-9-enamide (Compound 6).
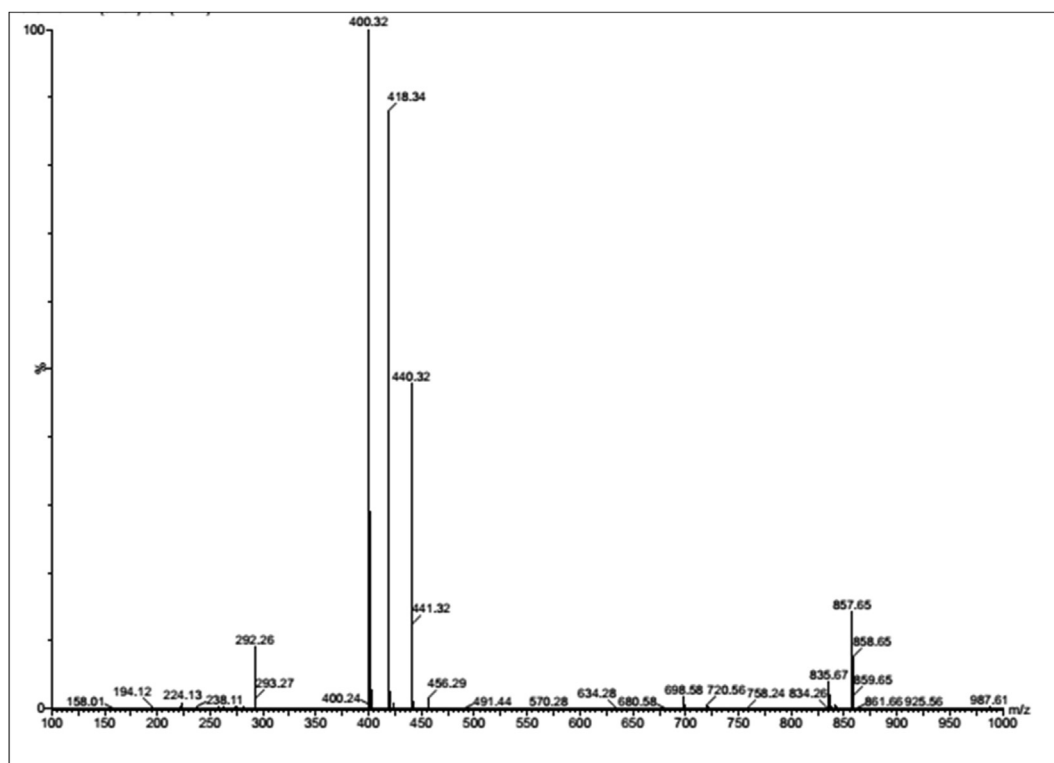
Figure 9. ESI-MS analysis of (*R,Z*)-12-hydroxy-*N*-(4-methoxybenzyl)octadec-9-enamide (Compound 6).

mechanically at room temperature until amide formation was completed. The side product *N,N*-dicyclohexylurea (DCU) was filtered off, and the filtrate was washed continuously with water (3 × 50 ml), 5% acetic acid, and then again with water (3 × 50 ml) and it is dried over anhydrous sodium sulphate. The solvent was removed under reduced pressure to give amides 5–7 (Figure 1). The compounds were purified over a column of silica gel using n-hexane-ethyl acetate (88:12, v/v) as an eluent. All these novel compounds were characterized by their spectral data.

2.3. N-(4-methoxybenzyl)undec-10-enamide

White amorphous compound 5, isolated yield, 90%, m.p, 91 °C, IR (KBr, cm^{-1}): 3302, 3078, 2920, 2851, 1638; ^{1}H NMR (400 MHz, δ ppm/CDCl$_3$): 7.17 (d, $J = 8.6$ Hz, 2H), 6.83 (d, $J = 8.6$ Hz, 2H), 6.08 (s, NH), 5.80 (m, 1H), 5.01–4.94 (dd, 2H), 4.32 (d, $J = 5.6$, 2H), 3.77 (s, 3H), 2.16 (t, 2H), 2.01 (m, 2H), 1.62 (m, 2H), 1.36 (m, 2H), 1.28 (m, 8H). ^{13}C NMR (100 MHz, δ ppm/CDCl$_3$): 173.07 (C), 158.92 (C), 139.15 (CH), 130.60 (CH), 129.12 (C), 114.18
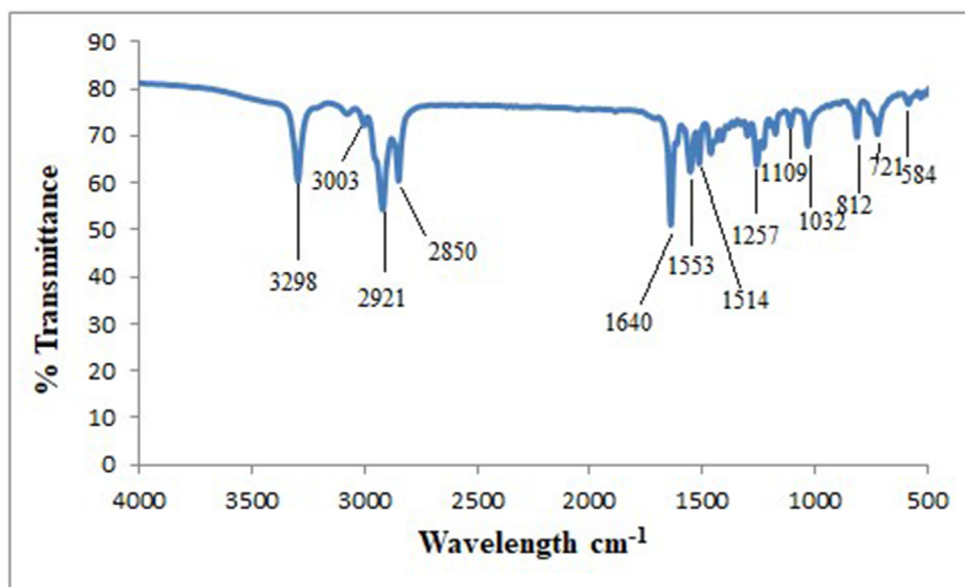

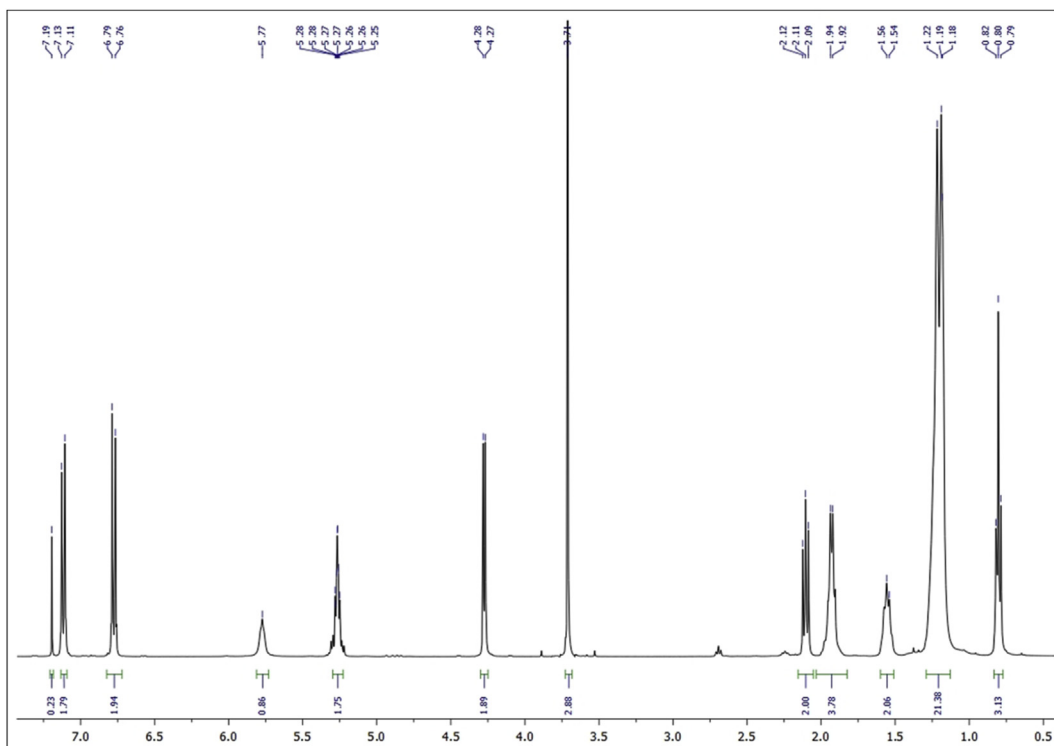**Figure 10.** FTIR analysis of *N*-(4-methoxybenzyl)oleamide (Compound 7).

Figure 11. ^{1}H NMR analysis of *N*-(4-methoxybenzyl)oleamide (Compound 7).

(CH$_2$), 113.99 (CH), 77.13 (CH$_3$), 55.26 (CH$_2$), 42.95 (CH$_2$), 36.73 (CH$_2$), 33.80 (CH$_2$), 29.71 (CH$_2$), 29.35 (CH$_2$), 29.08 (CH$_2$), 29.90 (CH$_2$), 25.80 (CH$_2$). ESI-MS for C$_{19}$H$_{29}$NO$_2$: calculated [M + H]$^+$: 304.23, found: 304.23.

2.4. (9Z, 12R)-12-hydroxy-N-(4-methoxybenzyl)octadec-9-enamide

White amorphous compound 6, isolated yield, 84%, m.p, 73 °C, IR (KBr, cm^{-1}): 3305, 3007, 2925, 2852, 1640; ^{1}H NMR (400 MHz, δ ppm/CDCl$_3$):
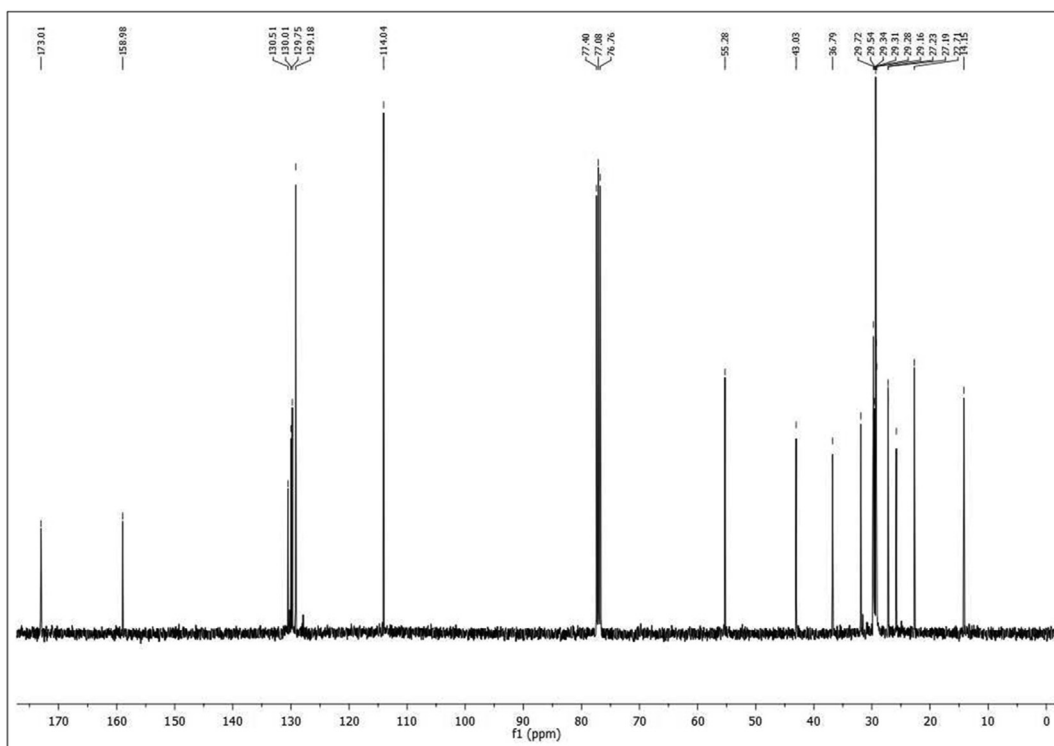

Figure 12. ^{13}C NMR analysis of *N*-(4-methoxybenzyl)oleamide (Compound 7).
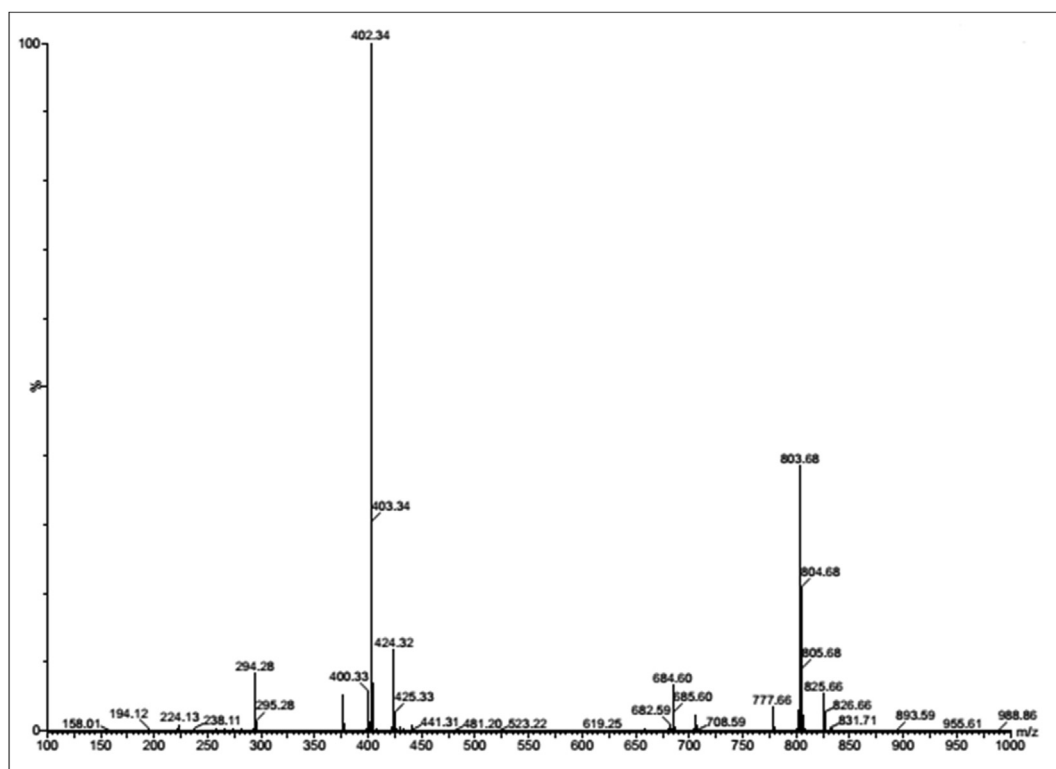
7

Figure 13. ESI-MS analysis of *N*-(4-methoxybenzyl)oleamide (Compound 7).
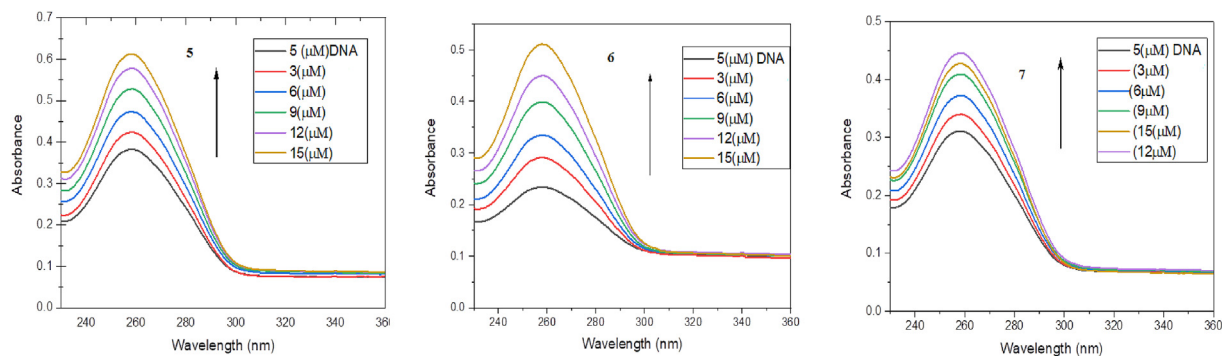

Figure 14. UV-vis absorption spectra of ctDNA in the absence and presence of varying concentration of compound 5: N-(4-methoxybenzyl)undec-10-enamide; 6: (9Z, 12R)-12-Hydroxy-*N*-(4-methoxybenzyl)octadec-9-enamide; 7: N-(4-methoxy benzyl)oleamide.

Table 1. The values of Stern–Volmer constant and quenching rate constant for the interaction of compounds with DNA.

pH	Compound	K_{sv} ($\times 10^3$ M^{-1})	K_q ($\times 10^{12}$ M^{-1} s^{-1})	R^2
7.4	Compound 5	6.04	6.04	0.9584
	Compound 6	5.14	5.14	0.9892
	Compound 7	5.44	5.44	0.9882

5: N-(4-methoxybenzyl)undec-10-enamide; 6: (9Z, 12R)-12-Hydroxy-*N*-(4-methoxybenzyl)octadec-9-enamide; 7: N-(4-methoxy benzyl)oleamide.

Table 2. The values of binding constant and the number of binding sites for the interaction of compounds with DNA.

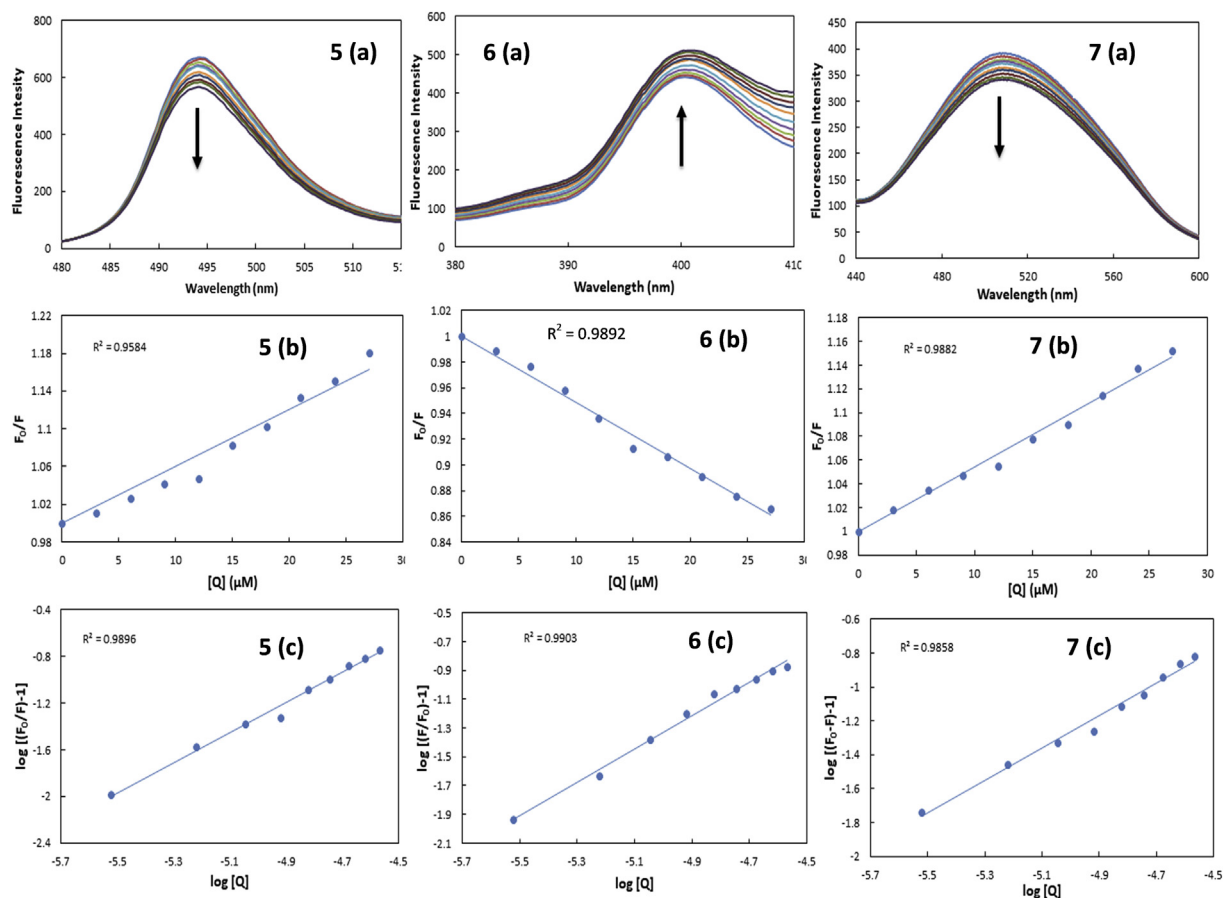| pH	Compound	K ($\times 10^4$ M^{-1})	n	R^2
7.4	Compound 5	14.46	1.29	0.9896
	Compound 6	2.87	1.15	0.9903
	Compound 7	0.3429	0.95	0.9858

5: N-(4-methoxybenzyl)undec-10-enamide; 6: (9Z, 12R)-12-Hydroxy-*N*-(4-methoxybenzyl)octadec-9-enamide; 7: N-(4-methoxy benzyl)oleamide.

Figure 15. Steady-state fluorescence spectra and Stern-volmer plots of compound 5 (a–c): N-(4-methoxybenzyl)undec-10-enamide; 6 (a–c): (9Z, 12R)-12-Hydroxy-*N*-(4-methoxybenzyl)octadec-9-enamide; 7 (a–c): N-(4-methoxy benzyl)oleamide in the absence and presence of varying concentration of ctDNA.
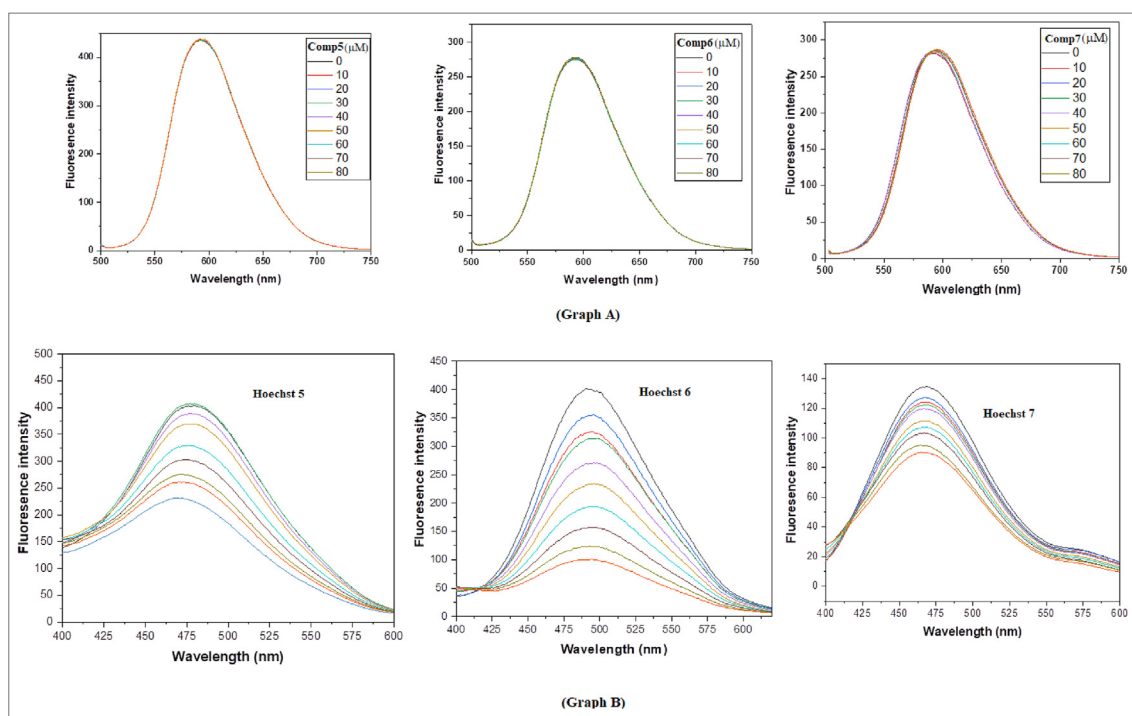
Figure 16. Competitive displacement assays. Graph A: Fluorescence titration of EB-DNA complex with increasing concentration of compound 5, 6 and 7, Graph B: Fluorescence titration of Hoechst-DNA complex with increasing concentration of compound 5: N-(4-methoxybenzyl)undec-10-enamide; 6: (9Z, 12R)-12-Hydroxy-*N*-(4-methoxybenzyl)octadec-9-enamide; 7: N-(4-methoxy benzyl)oleamide.

7.19 (d, *J* = 8.6, 2H), 6.85 (d, *J* = 8.6, 2H), 5.95 (s, NH), 5.55–5.50 (m, 1H), 5.42–5.36 (m, 1H), 4.34 (d, *J* = 5.6, 2H), 3.79 (s, 3H), 3.59 (m, 1H), 2.22–2.16 (m, 4H), 2.06–2.01 (m, 2H), 1.63 (t, 2H), 1.45 (m, 2H), 1.29 (m, 16 H), 0.88 (t, 3H). ^{13}C NMR (100 MHz, δ ppm/CDCl$_3$): 173.05 (C), 158.94 (C), 133.25 (CH), 130.54 (CH), 129.17 (C), 125.30 (CH), 114.02 (CH), 71.48 (CH), 55.28 (CH$_3$), 43.01 (CH$_2$), 36.83 (CH$_2$), 36.72 (CH$_2$), 35.35 (CH$_2$), 31.85 (CH$_2$), 29.55 (CH$_2$), 29.37 (CH$_2$), 29.21 (CH$_2$), 29.16 (CH$_2$), 29.07 (CH$_2$), 27.34 (CH$_2$), 25.73 (CH$_2$), 22.64 (CH$_2$), 14.12 (CH$_3$). ESI-MS for C$_{26}$H$_{44}$NO$_3$: calculated [M + H]$^+$: 418.33, found 418.34.

2.5. N-(4-methoxy benzyl)oleamide

Off white solid compound 7, isolated yield, 88%, m.p, 81 °C, IR (KBr, cm^{-1}): 3298, 3003, 2921, 2850, 1640; ^{1}H NMR (400 MHz, δ ppm/CDCl$_3$): 7.12 (d, *J* = 8.6 Hz, 2H), 6.77 (d, *J* = 8.6 Hz, 2H), 5.77 (s, NH), 5.28–5.25 (m, 2H), 4.27 (d, *J* = 5.6 Hz, 2H), 3.71 (s, 3H), 2.11 (t, 2H), 1.93 (m, 4H), 1.55 (m, 2H), 1.22–1.18 (m, 22H), 0.80 (t, 3H). ^{13}C NMR (100 MHz, δ ppm/CDCl$_3$): 173.01 (C), 158.98 (C), 130.51 (CH), 130.01 (CH), 129.75 (CH), 129.18 (C), 114.04 (CH), 77.13 (CH$_3$), 55.28 (CH$_2$), 43.03 (CH$_2$), 36.79 (CH$_2$), 31.92 (CH$_2$), 29.78 (CH$_2$), 29.72 (CH$_2$), 29.54 (CH$_2$), 29.34 (CH$_2$), 29.31 (CH$_2$), 29.28 (CH$_2$), 29.16 (CH$_2$), 27.21 (CH$_2$), 25.79 (CH$_2$), 22.71 (CH$_2$), 14.15 (CH$_3$). ESI-MS for C$_{26}$H$_{43}$NO$_2$: calculated [M + H]$^+$: 402.34, found 402.34.

3. DNA binding study

3.1. Sample preparation

The ctDNA purity was tested by observing the absorbance ratio at 260 and 280 nm (A 260/A 280) which was found to be 1.89, demonstrating that ctDNA was sufficiently free from molecule of protein (Mahadevan and Palaniandavar, 1998). By UV absorption at 260 nm, the ctDNA concentration in stock solution was observed to be 2.50×10-3 mol L^{-1} by using a molar absorption coefficient € 260 = 6600 L mol -1cm -1 (Kanakis et al., 2009).

3.2. UV-vis absorption spectral measurements

The UV-Vis spectra for all mixture solutions of ctDNA and compound 5, 6 and 7 were recorded from 230 to 350 nm using an UV-1800 spectrophotometer (Shimadzu, Japan) with a 1.0 cm quartz cuvette. The absorbance measurements were performed by keeping the DNA concentration constant (5 μM) while varying the 5, 6, and 7 concentrations (from 0-15 μM).

3.3. Fluorescence spectroscopic studies

The spectroflurophotometer (RF-5301PC Shimadzu, Japan) fitted with xenon flash lamp using 1.0 cm cell was used to carry out Fluorescence emission measurements of EDF. The fluorescence tests were obtained on Compounds 5, 6, and 7 at fixed concentrations (5 μM) with increasing ctDNA concentrations (0–45 μM). The fluorescence emission spectra were observed in wavelength 230–550 nm while exciting wavelength at 225 nm.

3.4. Competitive displacement assay

The EtBr displacement assay was performed on a solution EtBr (3 μM), ctDNA (5 μM) and different concentrations of compounds 5, 6, and 7. This complex (EtBr-ctDNA) was excited at 471 nm, with spectra of emissions were detected from 500 to 700 nm. Similarly, Hoechst 33342 dye displacement assays were carried with similar concentrations of dye and ctDNA like EtBr. However, the excitation and emission spectrum wavelength of ctDNA-Hoechst 3342 complex were commanded at 343 nm and 400–650 nm respectively.

3.5. Molecular docking study

The exert blind docking calculations between DNA sequence and compounds 5, 6 and 7 were performed by using MGL tools 1.5.4 with AutoGrid4 and AutoDock4. The sequence of DNA (CGCGAATTCGCG)2 used for the docking studies was obtained from Protein Data Bank (PDB ID: 1BNA). Chem Draw (2012) and OPLS-2005 force field were used to obtain the structures of compounds (5, 6, and 7) and 3D optimization (Hanwell et al., 2012), respectively. The water molecules were deleted at first sight. The DNA was surrounded in a box having grid points 76 × 78 × 120 in x × y × z directions and 0.375 Å as grind spacing. The AutoDock was used to obtain Lamarckian genetic algorithms, which were further employed to perform docking calculations. The rest of the parameters were of default settings. In all docking cases, the docked conformation with the lowest energy according to the Autodock scoring function was taken as binding mode. Moreover, PyMol molecular graphics program was used to obtain visualization of the docked pose.

4. Antimicrobial studies

4.1. Antimicrobial activity

Minimum inhibitory concentration (MIC) was estimated by the micro-broth dilution method, according to the British Society for Antimicrobial Chemotherapy (BSAC) guidelines (Ghosh et al., 2015). The selective bacteria *E. Coli* and *Agrobacterium tumefaciens* (*A. tumefaciens*) and fungi (*Alternaria* and *Rhizopus*) were applied to assess the antimicrobial potency of compound 5, compound 6, and compound 7 with different concentrations (Das et al., 2010). Subculturing of the bacteria and fungi was carried out at 37 °C for overnight, and turbidity of Macfarland standard No. 0.5 was used to evaluate the growth of the selected microbes. The assay was performed in three replicates, and the MIC and MKC were determined after 24 h of the prepared samples (Senthil and Kamaraj, 2011).

4.2. Disc diffusion assay

The antimicrobial activity of prepared samples was carried out with disc diffusion method against to *E. Coli, A. tumefaciens, Alternaria* and *Rhizopus* on nutrient agar (NA) plate (Zare et al., 2018). Microbial suspension in Luria broth (concentration of 120 ml-1 of each microbe) from freshly prepared cultures was used as working suspension. From each bacterial culture, about 20 μl (120 CFU ml-1) were spreaded on the agar surface by sterile glass beads. The discs with 6 mm diameter were placed on agar plates. As a positive control, antibiotic/antifungal Kanamycin/Amphotericin was used and a paper disc without coatings was used as a control. The plates were incubated at 37 C for 24 h for bacterial culture and 32 h for fungal culture. The antimicrobial activity was assessed by determining the diameter of the zone of inhibition against the microbes.

5. Results and discussion

5.1. Chemistry

There is the latest trend to use catalysts in organic reactions to improve yields, shorten reaction times as well as promoting multiple preferred routes for new reactions. To exploit the probability to find new compounds which are pharmacologically active, our focus has turned to use of catalysts. In most of the synthesized compounds, the yield of the product was 84–90%. The amidification of PMBA with undec-10-enoic acid was taken as a model to adjust the conditions for the preparation of compounds 5–7 (Figure 1). In order to optimize the reaction conditions for fatty acid amide synthesizes, variation of molar ratios of reagents and catalysts were performed. After numerous experiments, we found a set of conditions that yields better results and thus optimum conditions for molar ratio of FA, MBA, DCC, and DMAP were set up. All the newly synthesized compounds were characterized by IR, 1H NMR, 13C NMR
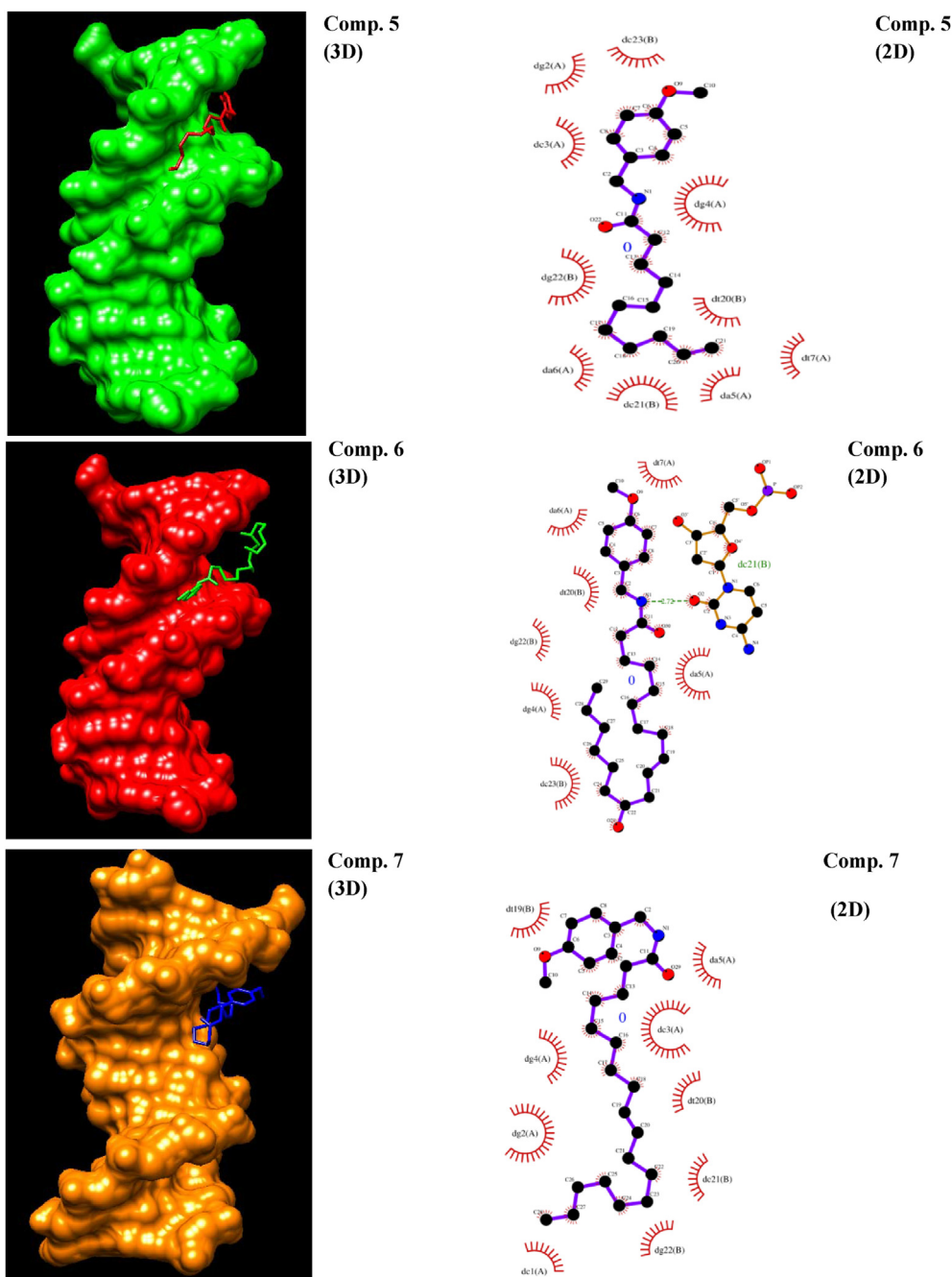
Figure 17. Molecular docked structures of compound 5: N-(4-methoxybenzyl)undec-10-enamide; 6: (9*Z*, 12*R*)-12-Hydroxy-*N*-(4-methoxybenzyl)octadec-9-enamide; 7:N-(4-methoxybenzyl)oleamide complexed with DNA. Figures represents minor groove binding of compound 5, 6 and 7 with dodecamer d(CGCGAATTCGCG) 2 (PDB ID: 1BNA).

and mass spectra data as given in (Figures 2, 3, 4, 5, 6, 7, 8, 9, 10, 11, 12, and 13). IR absorptions characteristics of amide (1638-1640 cm-1) were observed in all the synthesized compounds. N-(4-methoxybenzyl)undec-10-enamide compound 5 showed characteristic IR bands at 3302 (NH) and 1638 cm-1 (C=O, amide). 1H NMR was more supportive in assigning the structure showing peaks at δ 6.08 (s, NH). In 13C NMR peaks at 173.07 (C), 158.92 (C), 139.15 (CH), 130.60 (CH), 129.12 (C) and 114.18 (CH2) were observed. Mass spectral data [m/z = 304.23 (M + H)+] showed its characterized molecular ion peak in accordance with the molecular formula (C19H29NO2). Similarly, other compounds were characterized from their spectra data.

5.2. UV-vis spectroscopic studies

The binding of compounds 5, 6, and 7 to ctDNA has been studied through the changes in absorbance and wavelength shifts. The absorption band at 260 nm of DNA arises due to p–p* transition of nitrogen bases present in DNA. Absorption spectra were recorded at room temperature using a standard quartz cell having path length of 1.0 cm, in which 2.0 mL of 5 μM DNA solution was placed. With the gradual addition of 5, 6, and 7 (3–15 μM) to the fixed concentration of ctDNA (5 μM) a continuous increase of the absorption spectrum of ctDNA was apparent (Figure 14).

Table 3. Binding energies of different compounds with obtained using AutoDock 4.

S. No	Compound	Binding Energy (kcal mol^{-1})
1	Compound 5	-5.21
2	Compound 6	-3.55
3	Compound 7	-3.91

5: N-(4-methoxybenzyl)undec-10-enamide; 6: (9Z, 12R)-12-Hydroxy-N-(4-methoxybenzyl)octadec-9-enamide; 7: N-(4-methoxy benzyl)oleamide.

5.3. Fluorescence studies

Dynamic and static quenching are the two modes by which quenching can arise. In dynamic quenching, the quencher in very short existence comes in contact with excited state, while as in static quenching there is the formation of fluorophore–quencher complex. In general, dynamic and static quenching depends on excited-state lifetime and temperature. On increase in temperature, dynamic quenching increases because compounds have to move fast in this condition which causes more probability of collisions. Static quenching mainly occurs due to composite formation. Hence on increasing the temperature, the stability of the composite decreases, which ultimately leads to fluorescence quenching descending (Guo et al., 2007). So in both cases, the concentration of the quencher determines the fluorescence intensity and the quenched fluorophore can be used as an indicator for the quenching agent (Berlman, 1971).

Fluorescence quenching is described by the Stern–Volmer equation Eq. (1):

$$F0/F = 1 + Kq \, 0 \, Q = 1 + K \, svQ \tag{1}$$

where F_0 and F represent the fluorescence intensities in the absence and in the presence of used quencher (DNA), respectively. Kq is the fluorophore quenching rate constant, K sv is quenching constant, 0 is the lifetime of the fluorophore in the absence of a quencher (0 = 10-8), and [Q] is the concentration of quencher (Zhou et al., 2007). The values are given in Table 1.

The binding constant (Kf) and the binding stoichiometry (n) as given in (Table 2) for the formation of a complex between DNA and adefovir dipivoxil were analyzed (Gosselin et al., 1994) by using Eq. (2):

$$Log(F0 - F/F) = LogKf + nlog|Q| \tag{2}$$

Where, F and F0 are fluorescence intensities of the fluorophore in the presence and absence of varying concentrations of ctDNA, respectively, n is equivalent binding site number, and the slope based on the Eq. (2) and given in (Figure 15) revealed it.

5.4. Competitive displacement analysis
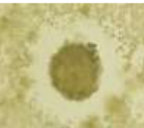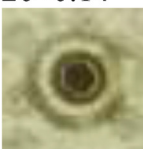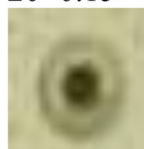
The fluorescent DNA probe was used to study the mode of binding between small molecules with ctDNA and their way of bindings was well recognized. It was observed that if a molecule binds with ctDNA substitutes a bound dye, then it is thought that it would bind to the ctDNA in a similar fashion as that of dye (Song et al., 2000). The EtBr is one of the most delicate dye that can bind to ctDNA with intense fluorescence due to its strong intercalation mode (Liu and Sadler, 2011; Zhang et al., 2013). From Figure 16, it is clear that the addition of compounds 5, 6 and 7 to the ctDNA + EtBr complex does not show any substantial change in the fluorescence intensity hence rules out any possibility of intercalative mode of binding with compounds 5, 6 and 7.

Hoechst 33342, a well-established minor groove binder of ctDNA, was taken as a molecular probe to confirm mode of binding between
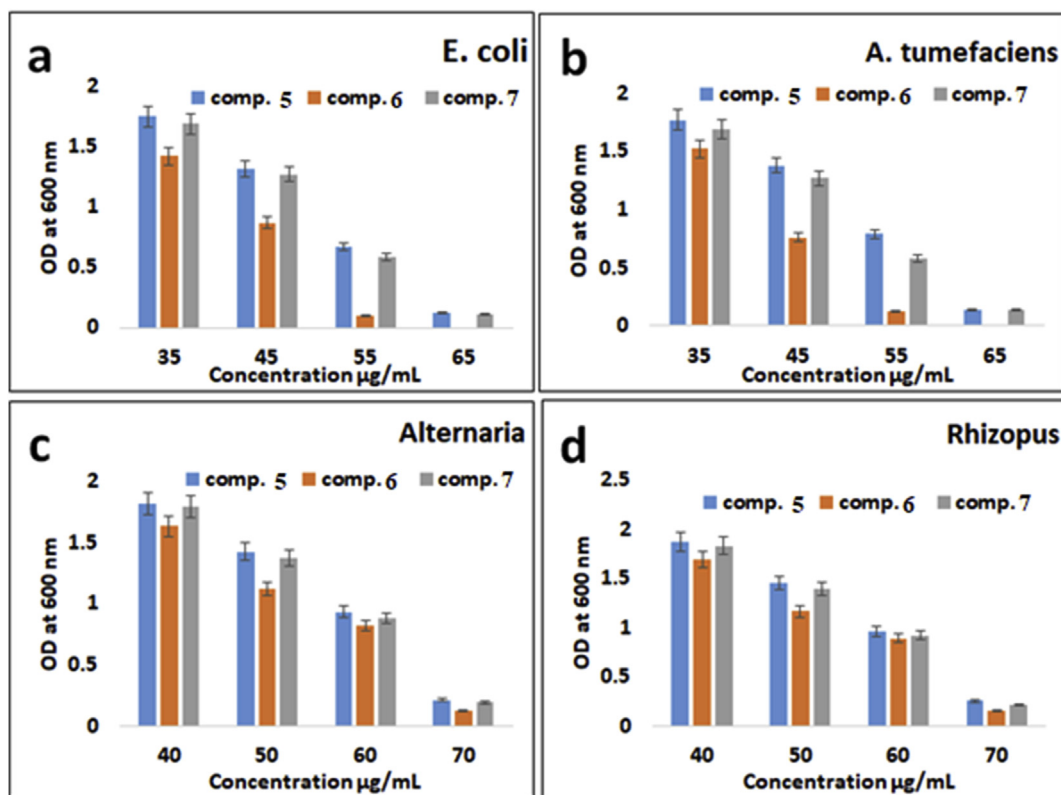
Figure 18. Effect of different concentrations of comp. 5: N-(4-methoxybenzyl)undec-10-enamide; 6: (9Z, 12R)-12-Hydroxy-N-(4-methoxybenzyl)octadec-9-enamide; 7: N-(4-methoxy benzyl)oleamide on growth of (a) *E. Coli,* (b) *A. tumefaciens,* (c) *Alternaria* and (d) *Rhizopus.*

Sample (20 µg ml⁻¹)	Zone of Inhibition (in mm)			
	E. Coli	*A. tumefaciens*	*Alternaria*	*Rhizopus*
Comp. 5	14±0.16	15±0.19	14±0.13	13±0.21
Comp. 6	18±0.15	19±0.18	17±0.16	15±0.24
Comp. 7	17±0.21	18±0.23	16±0.19	12±0.14
Kanamycin/ Amphotericin	20±0.14	22±0.12	18±0.13	20±0.15

Figure 19. Inhibition on growth of bacteria (*E. Coli* and *A. tumefaciens*) and fungi (*Alternaria* and *Rhizopus*) with the 5: N-(4-methoxybenzyl)undec-10-enamide; 6: (9*Z*, 12*R*)-12-Hydroxy-*N*-(4-methoxybenzyl)octadec-9-enamide; 7: N-(4-methoxy benzyl)oleamide and Kanamycin/Amphotericin (measurement of zone of inhibition).

compounds–ctDNA systems (Manna and Chakravorti, 2012; LePecq and Paoletti, 1967) Hoechst 33342, which can powerfully bind with ctDNA and increase its intensity of fluorescence (Yaseen et al., 2014). As displayed in (Figure 16) on the addition of compounds 5, 6 and 7 to DNA + Hoechst 33342 systems, the emission intensities of Hoechst 33342-DNA solution were found to decrease. This indicates that compounds 5, 6 and 7 binds to the ctDNA by binding to the minor groove of the ctDNA.

5.5. Molecular docking analysis

Molecular docking is an important technique by which we can understand the interactions of drug-DNA. Moreover, it helps to study an efficient approach by keeping a small molecule into the DNA at its binding site mainly in a non-covalent fashion, although covalent bond may also be constituted with reactive ligand (Haq and Ladbury, 2000). Different structural properties of molecules lead to different binding modes; in fact, one of the most critical factors governing the binding mode is the molecular shape (Proudfoot et al., 2001; Arjmand et al., 2012). In this experimental study, the studied compounds were successively docked with duplex DNA that follows the sequence d(CGCGAATTCGCG)2 dodecamer (PDB ID: 1BNA) so as to expect the possible binding site and suitable orientation of the compound inside the DNA groove. The promising conformation of the docked pose confirmed that compounds 5, 6 and 7 binds to DNA groove (Figure 17).

From the data of docking calculation, the minimum binding energy conformer is selected up from 1 minimum energy conformer from the 50 runs. The run data for the conformers are displayed in Table 3. According to the energetically favorable conformation of the docked pose (Figure 17) confirmed that compounds 5, 6, and 7 binds to DNA minor groove and is located within narrower A–T (10.8 Å) regions as

compared to G–C (13.2 Å) ones. This is mainly due to better binding of adefovir bearing benzyl moiety to A–T regions compared to the G–C region, which defines the stability of groove mainly due to hydrophobic contacts and van der Waals interactions with functional groups of the DNA.

It had been observed From the docking simulation the binding free energy change (DG) of the drug-DNA complex was calculated to be -5.21 kcal mol-1 which is higher as related to free binding energy (-4.90 kcal mol-1) obtained experimentally from the fluorescence data. This difference in free energy changes might be due to the solvent exclusion and/or rigidity of some other receptor DNA in the study of molecular docking. Moreover, from UV–visible method, the binding constant obtained was correlated with the free binding energy of docked model.

5.6. Antimicrobial activity

The antimicrobial potency of compounds 5, 6 and 7 were validated by inhibiting the growth of bacteria and fungi under a potential mechanism of physical interaction of compounds with microbes. The study was carried out using selective bacterial and fungal pathogens, and Figure 18 displays the effect of different concentrations of these compounds on the growth of (a) *E. Coli,* (b) *A. tumefaciens,* (c) *Alternaria,* and (d) *Rhizopus.* Minimum Inhibitory Concentration (MIC) and Minimum Killing Concentration (MKC) values for the compounds 5, 6, and 7 were estimated by analyzing the growth of *E. Coli, A. tumefaciens, Alternaria,* and *Rhizopus.* Visual turbidity analysis displayed the inhibiting concentration of comp. 6 was 45 µg/ml for bacteria and 70 µg/ml for fungi whereas, comp. 5 and 7 were displayed at 55 µg/ml for bacteria and 70 µg/ml for fungi and considered as MIC values. After re-inoculation with different concentrations of these compounds (5, 6, and 7), no growth was observed as

above mentioned concentrations for respective bacteria and fungi, and they were considered as MKC values also.

5.7. Disc diffusion assay

Qualitative assessment of antimicrobial activity was performed by the disc diffusion method. A comparative study of inhibition zones was made after measuring the diameter of inhibition zones. As given in (Figure 19), Comp. 6 showed a higher effect for both bacteria and fungi than comp. 5 and 7, which was found to be similar with an earlier study (Farshori et al., 2010). Among all combinations, comp. 6 against to *A. tumefaciens* (bacteria) and comp. 6 against *Alternaria* (fungi) displayed higher effect whereas comp. 5 against *E. Coli* (bacteria) and comp. 7 against *Rhizopus* (fungi) displayed the lowest effect. Experiments were carried out in three replicates, and the outcome results were displayed as a mean of the replicates with standard deviation (Figure 19).

6. Conclusion

In summary, the proposed synthetic method is simple, sustainable and quantitative. Moreover, the study revealed the interaction of the compounds 5, 6, and 7 binding modes with ctDNA by multispectroscopic techniques and molecular modeling study. Hyperchromism shift was observed upon addition of various concentrations of DNA in all compounds, which suggests the strong interaction between compounds 5, 6, and 7 and DNA. The fluorescence assay presented that the emission intensity of the drug was quenched by the addition of DNA. This quenching mechanism is described by photoelectron transfer from DNA (guanine base) to various excited levels of synthesized compounds. The free energy values of compounds 5, 6 and 7 are negative at various temperatures, which clearly indicate the spontaneity of compounds 5, 6, and 7 with DNA binding. The results conceal that the most important contributions to the binding process are hydrophobic interactions. The docking outcomes confirmed that groove mechanism is followed by compounds 5, 6 and 7 to bind with DNA. Moreover, the variability of antimicrobial activity of these compounds especially compound 6 is a strong validation of this study. These findings provide a broad biochemical base for improving the antimicrobial potency of these compounds in drug design and development in the future.

Declarations

Author contribution statement

Zubair Rehman Nengroo: Conceived and designed the experiments; Performed the experiments; Analyzed and interpreted the data; Wrote the paper.

Aijaz Ahmad: Performed the experiments; Contributed reagents, materials, analysis tools or data; Wrote the paper.

Adil Tantary: Conceived and designed the experiments; Performed the experiments; Analyzed and interpreted the data; Wrote the paper.

Adil Shafi Ganie: Analyzed and interpreted the data; Wrote the paper.

Zeshan Umar Shah: Contributed reagents, materials, analysis tools or data; Wrote the paper.

Data availability statement

Data included in article/supp. material/referenced in article.

Declaration of interests statement

The authors declare no conflict of interest.

Additional information

No additional information is available for this paper.

References

Adelani, A.K., Labunmi, L., 2017. Characterization and biological activities of fatty acid amides synthesized from four underutilized plant seed oils. J. Chem. Pharm. Res. 9, 18–23.

Ahmad, A., Ahmad, A., Varshney, H., Rauf, A., Rehan, M., Subbarao, N., Khan, A.U., 2013. Designing and synthesis of novel antimicrobial heterocyclic analogs of fatty acids. Eur. J. Med. Chem. 70, 887–900.

Ahn, K., Johnson, D.S., Cravatt, B.F., 2009. Fatty acid amide hydrolase as a potential therapeutic target for the treatment of pain and CNS disorders. Expet Opin. Drug Discov. 4, 763–784.

Arjmand, F., Parveen, S., Afzal, M., Toupet, L., Hadda, T.B., 2012. Molecular drug design, synthesis and crystal structure determination of CuII–SnIV heterobimetallic core: DNA binding and cleavage studies. Eur. J. Med. Chem. 49, 141–150.

Banday, M.R., Farshori, N.N., Ahmad, A., Khan, A.U., Rauf, A., 2010. Synthesis and characterization of novel fatty acid analogs of cholesterol: in vitro antimicrobial activity. Eur. J. Med. Chem. 45, 1459–1464.

Berlman, L.B., 1971. Handbook of Fluorescence Spectra in Aromatic Molecules. Academic Press, New York.

Das, K., Tiwari, R.K.S., Shrivastava, D.K., 2010. Techniques for evaluation of medicinal plant products as antimicrobial agent: current methods and future trends. J. Med. Plants Res. 4, 104–111.

Devasia, R.A., Jones, T.F., Ward, J., Stafford, L., Hardin, H., Bopp, C., Beatty, M., Mintz, E., Schaffner, W., 2006. Endemically acquired foodborne outbreak of enterotoxin-producing Escherichia coli serotype O169: H41. Am. J. Med. 119, 168 e7.

Di Marzo, V., Bisogno, T., De Petrocellis, L., 2007. Endocannabinoids and related compounds: walking back and forth between plant natural products and animal physiology. Chem. Bio. 14, 741–756.

Fernandez, L.R., Svetaz, L., Butassi, E., Zacchino, S.A., Palermo, J.A., Sanchez, M., 2016. Synthesis and antifungal activity of bile acid-derived oxazoles. Steroids 108, 68–76.

Farshori, N.N., Banday, M.R., Zahoor, Z., Rauf, A., 2010. DCC/DMAP mediated esterification of hydroxy and non-hydroxy olefinic fatty acids with β-sitosterol: in vitro antimicrobial activity. Chin. Chem. Lett. 21, 646–650.

Felder, C.C., Dickason-Chesterfield, A.K., Moore, S.A., 2006. Cannabinoids biology: the search for new therapeutic targets. Mol. Interv. 6, 149.

Ghosh, T., Das, A.B., Jena, B., Pradhan, C., 2015. Antimicrobial effect of silver zinc oxide (Ag-ZnO) nanocomposite particles. Front. Life Sci. 8, 47–54.

Gosselin, G., Imbach, J.L., Sommadossi, J.P., 1994. Antiviral nucleoside analogues and their bioactive phosphorylated metabolites: state of the art review of their detection and tissue monitoring applied to the anti-HIV drug AZT. Bull. Inst. Pasteur. 92, 181–196.

Gunstone, F.D., 1954. Fatty acids. Part II. The nature of the oxygenated acid present in Vernonia anthelmintica (Willd.) seed oil. J. Chem. Soc. 1611–1616.

Guo, L., Qiu, B., Chen, G., 2007. Synthesis and investigation on the interaction with calf thymus deoxyribonucleic acid of a novel fluorescent probe 7-oxobenzo [b][1, 10] phenanthroline-12 (7H)-sulfonic acid. Anal. Chim. Acta 588, 123–130.

Hanwell, M.D., Curtis, D.E., Lonie, D.C., Vandermeersch, T., Zurek, E., Hutchison, G.R., 2012. Avogadro: an advanced semantic chemical editor, visualization, and analysis platform. J. Cheminf. 4, 17.

Haq, I., Ladbury, J., 2000. Drug–DNA recognition: energetics and implications for design. J. Mol. Recogn. 13, 188–197.

Kanakis, C.D., Nafisi, S., Rajabi, M., Shadaloi, A., Tarantilis, P.A., Polissiou, M.G., Bariyanga, J., Tajmir-Riahi, H.A., 2009. Structural analysis of DNA and RNA interactions with antioxidant flavonoids. J. Spectrosc. 23, 29–42.

Karanian, D.A., Bahr, B.A., 2006. Cannabinoid drugs and enhancement of endocannabinoid responses: strategies for a wide array of disease states. Curr. Mol. Med. 6, 677–684.

Kathiravan, A., Renganathan, R., 2009. Photoinduced interactions between colloidal TiO2 nanoparticles and calf thymus-DNA. Polyhedron 28, 1374–1378.

LePecq, J.B., Paoletti, C.A., 1967. Fluorescent complex between ethidium bromide and nucleic acids: physical—chemical characterization. J. Mol. Biol. 27, 87–106.

Li, B., Webster, T.J., 2018. Bacteria antibiotic resistance: new challenges and opportunities for implant-associated orthopedic infections. J. Orthop. Res. 36, 22–32.

Liu, H.K., Sadler, P.J., 2011. Metal complexes as DNA intercalators. Acc. Chem. Res. 44, 349–359.

Mahadevan, S., Palaniandavar, M., 1998. Spectroscopic and voltammetric studies on copper complexes of 2, 9-dimethyl-1, 10-phenanthrolines bound to calf thymus DNA. Inorg. Chem. 37, 693–700.

Manna, A., Chakravorti, S., 2012. Modification of a styryl dye binding mode with calf thymus DNA in vesicular medium: from minor groove to intercalative. J. Phys. Chem. B 116, 5226–5233.

Nengroo, Z.R., Rauf, A., 2019. Fatty acid composition and antioxidant activities of five medicinal plants from Kashmir. Ind. Crop. Prod. 140, 111596.

Nengroo, Z.R., Rauf, A., 2020. Inula racemosa and Digitalis purpurea from Kashmir: fatty acid composition, antioxidant, antibacterial activities, and functional group evaluation. Flavour Fragrance J. 35, 653–665.

Nengroo, Z.R., Rauf, A., Danish, M., Dar, M.S., 2020. Evaluation of fatty acid composition and antimicrobial activity of eight medicinal plants from Kashmir. Orient. J. Chem. 36, 44–53.

Nolan, C.M., Chalhub, E.G., Nash, D.G., Yamauchi, T., 1979. Treatment of bacterial meningitis with intravenous amoxicillin. Antimicrob. Agents Chemother. 16, 171–175.

Proudfoot, E.M., Mackay, J.P., Karuso, P., 2001. Probing site specificity of DNA binding metallointercalators by NMR spectroscopy and molecular modeling. Biochem 40, 4867–4878.

Puerto, A.S., Fernández, J.G., Del Castillo, J.D.D.L., Pino, M.J.S., Angulo, G.P., 2006. In vitro activity of β-lactam and non–β-lactam antibiotics in extended-spectrum β-lactamase–producing clinical isolates of Escherichia coli. Diagn. Microbiol. Infect. Dis. 54, 135–139.

Ramachandran, G., 2014. Gram-positive and gram-negative bacterial toxins in sepsis: a brief review. Virulence 5, 213–218.

Saquib, Q., Al-Khedhairy, A.A., Alarifi, S.A., Dutta, S., Dasgupta, S., Musarrat, J., 2010. Methyl thiophanate as a DNA minor groove binder produces MT–Cu (II)–DNA ternary complex preferably with AT rich region for initiation of DNA damage. Int. J. Biol. Macromol. 47, 68–75.

Senthil, K.S., Kamaraj, M., 2011. Antimicrobial activity of Cucumis anguria L. by agar well diffusion method. Bot. Res. Int. 4, 41–42.

Shafiei, M., Peyton, L., Hashemzadeh, M., Foroumadi, A., 2020. History of the development of antifungal azoles: a review on structures, SAR, and mechanism of action. Bioorg. Chem. 104, 104240.

Sheehan, J.C., Hess, G.P., 1955. A new method of forming peptide bonds. J. Am. Chem. Soc. 77, 1067–1068.

Song, Y., Kang, J., Zhou, J., Wang, Z., Lu, X., Wang, L., Gao, J., 2000. Study on the fluorescence spectra and electrochemical behavior of ZnL2 and Morin with DNA. Spectrochim. Acta Part A: Spectrochim. Acta A. 56, 2491–2497.

Starowicz, K., Nigam, S., Di Marzo, V., 2007. Biochemistry and pharmacology of endovanilloids. Pharmacol. Ther. 114, 13–33.

Tan, J., Wang, B., Zhu, L., 2009. DNA binding, cytotoxicity, apoptotic inducing activity, and molecular modeling study of quercetin zinc (II) complex. Bioorg. Med. Chem. 17, 614–620.

Tjahjono, D.H., Akutsu, T., Yoshioka, N., Inoue, H., 1999. Cationic porphyrins bearing diazolium rings: synthesis and their interaction with calf thymus DNA. Biochim. Biophys. Acta 1472, 333–343.

Witkamp, R.F., 2010. Biologically active compounds in food products and their effects on obesity and diabetes. Comp. Nat. Prod. II: Chem. Bio. 509–545.

Yaseen, Z., Banday, A.R., Hussain, M.A., Tabish, M., 2014. Determination of the cationic amphiphilic drug–DNA binding mode and DNA-assisted fluorescence resonance energy transfer amplification. Spectrochim. Acta Part A: Spectrochim. Acta. A 122, 553–564.

Yoder, J.S., Cesario, S., Plotkin, V., Ma, X., Shannon, K.K., Dworkin, M.S., 2006. Outbreak of enterotoxigenic Escherichia coli infection with an unusually long duration of illness. Clin. Infect. Dis. 42, 1513–1517.

Zare, M., Namratha, K., Thakur, M.S., Yallappa, S., Byrappa, K., 2018. Comprehensive biological assessment and photocatalytic activity of surfactant assisted solvothermal synthesis of ZnO nanogranules. Mater. Chem. Phys. 215, 148–156.

Zhang, G., Hu, X., Fu, P., 2012. Spectroscopic studies on the interaction between carbaryl and calf thymus DNA with the use of ethidium bromide as a fluorescence probe. J. Photochem. Photobiol. B Biol. 108, 53–61.

Zhang, J., Cai, D., Wang, S., Tang, Y., Zhang, Z., Liu, Y., Gao, X., 2014. Efficient method for the synthesis of fatty acid amide from soybean oil methyl ester catalysed by modified CaO. Can. J. Chem. Eng. 92, 871–875.

Zhang, W., Berberov, E.M., Freeling, J., He, D., Moxley, R.A., Francis, D.H., 2006. Significance of heat-stable and heat-labile enterotoxins in porcine colibacillosis in an additive model for pathogenicity studies. Infect. Immun. 74, 3107–3114.

Zhang, Y., Zhang, G., Li, Y., Hu, Y., 2013. Probing the binding of insecticide permethrin to calf thymus DNA by spectroscopic techniques merging with chemometrics method. J. Agric. Food Chem. 61, 2638–2647.

Zhou, N., Liang, Y.Z., Wang, P., 2007. 18β-Glycyrrhetinic acid interaction with bovine serum albumin. J. Photochem. Photobiol. A 185, 271–276.